RSC Advances

Journal Name

COMMUNICATION

Dramatic daylight induced photocatalytic performance of carbon quantum dots decorated N-doped ZnO with suppressed photocorrosion

Muthulingam[a], Kang Bin Bae[b], Rizwan Khan[b], In-Hwan Lee[b,*], and Periyayya Uthirakumar [a,b,*]

Carbon quantum dots decorated N-doped ZnO (CQD/N-ZnO) composites were prepared as a promising strategy to enhance the photocatalytic performance on aqueous malachite green (MG) dye. It was found that the primary role of CQD is to enhance the visible light absorption efficiency and an effective separation of photo-generated electron-hole pairs along with the suppressed photocorrosion of ZnO crystals.

The progress towards the development of efficient photocatalyst is a critical issue for an environmental remediation due to major organic contaminants originated from the textile and food industries. Various inorganic semiconductors are recommended to use as a photocatalyst to decrease the environmental impacts due to its efficiency and broad applicability. Amongst, zinc oxide (ZnO) is blooming nowadays as of being its high catalytic activity, low cost, wide band gap (3.37 eV) and environmental friendliness over other photocatalysts [1]. However, a quick recombination of photo-generated electron–hole pairs and the narrow absorption band of the ZnO photocatalyst are the major concerns that affect their photocatalytic efficiency. To overwhelm these issues, a suitable modification is obligatory for developing new types of ZnO nanostructures by incorporating either secondary semiconductor metal [2] or carbon nanoparticle [3-9]. Also, nitrogen doping is one way to alter the band gap energy of ZnO to improve the charge separation efficiency of photocatalyst [10]. For example, doping of nitrogen, an anion element with small radii, could be easily incorporated into the lattice of ZnO by replacing the O atoms or occupying the interstitial sites. Thus, it extends their light harvest tendency at the higher wavelength region [10,11].

Carbon quantum dots (CQDs) have received the considerable attention in the recent past owing to their advantages in non-toxic, photostability, low cost, heavy metal-free and eco-friendly over traditional toxic heavy-metal based quantum dots creating serious health and environmental issues [11]. Although, several works have been reported on using C-60, graphene and carbon nanofiber as electron scavenging agents [3,6,7], it was rare work involved in synthesizing the photocatalysts with CQDs [5]. In general, CQD had established the characteristics of photo-induced electron transfer properties [7] and up-conversion of PL properties [5] over other carbon based structures. Thus, the combination of N-doped ZnO and CQD seems to be an ideal tactic for endorsing the improvement of charge separation by hindering charge recombination to enhance the photocatalytic efficiency along with anti-photocorrosion. Besides, in case of industrial perspective, it is inevitable that at least a specific light source apparently required (UV or visible light) to treat a huge volume of industrial wastewater. Obviously, it is often expensive to provide such a specific light source for treating large quantity of wastewater in industry. Hence, utilization of naturally available daylight source will be a better alternative way to degrade the dye molecules in large scale. Herein, we report an easy methodology for preparing N-doped ZnO, CQDs, and CQDs decorated N-ZnO (CQD/N-ZnO), exhibiting an enhanced photocatalytic activity on MG dye under different light sources. We have given more preference to evaluate the photocatalytic performance of CQD/N-ZnO composite under the naturally available direct daylight irradiation as of industrial perspective.

Detailed synthesis, characterization and photocatalytic investigations are disclosed in the Electronic Supplementary Information (see ESI). The crystal structure and phase composition of N-doped ZnO and CQD/N-ZnO composites were revealed by X-ray diffraction (XRD) analysis. Fig. 1 shows the XRD patterns of N-doped ZnO and CQD/N-ZnO composites. The XRD spectrum of N-doped ZnO was well-crystallized and the diffraction peaks could be perfectly indexed to the hexagonal phase ZnO (JCPDS No. 79-0206). The primary diffraction peaks appeared at 2θ values of 31.7°, 33.4° and 36.2°, representing (100), (002) and (101) assigned crystal planes of ZnO [12]. While for the CQD/N-ZnO composite, notably, a broader diffraction peak at near 26° attributing to graphitic (002) peak evidently appears along with a slight shift (36.21° to 36.08°) in (002) diffraction peak, as clearly seen in the enlarged XRD patterns between 35° and 40° (Fig. 1b), indicating that the CQDs were successfully coated on ZnO surface [4]. However, no obvious

deviations assigned to nitrogen doping was detected in XRD patterns. Hence, X-ray photoelectron spectroscopy (XPS) was performed to investigate the chemical state and surface composition of powder samples. Fig. 1c-d shows the XPS survey scan and the high-resolution XPS spectra core level N 1s scan of CQD/N-ZnO. The full XPS survey scan of the CQD/N-ZnO exhibited the peaks that were assignable to Zn, O, C and N. The core level high resolution N 1s spectrum (Fig. 1d) shows that peaks appeared at 396.1, 397.2, 398.8, and 400.1 eV, which indicated that the nitrogen was incorporated into ZnO crystals. The major peak appeared at 396.1 eV is assigned to -N-Zn-N- bond and the peak at 397.2 eV may be assigned to -N-C- bond [13]. The other two peaks at 398.8 eV and 400.1 eV can be assigned to -N-H- bond and –O-Zn-N-, respectively [13,14]. The detailed high resolution XPS spectra of Zn 2p, C 1s and O 1s core level scans can be seen in the supporting information (Fig. S1). The existence of CQD and ZnO phases in CQD/N-ZnO composite was further confirmed by nano-Raman, UV-vis spectra, Fourier transform infrared (FT-IR), energy dispersive spectroscope (EDS) and high resolution transmission electron microscopy (HRTEM) investigations.
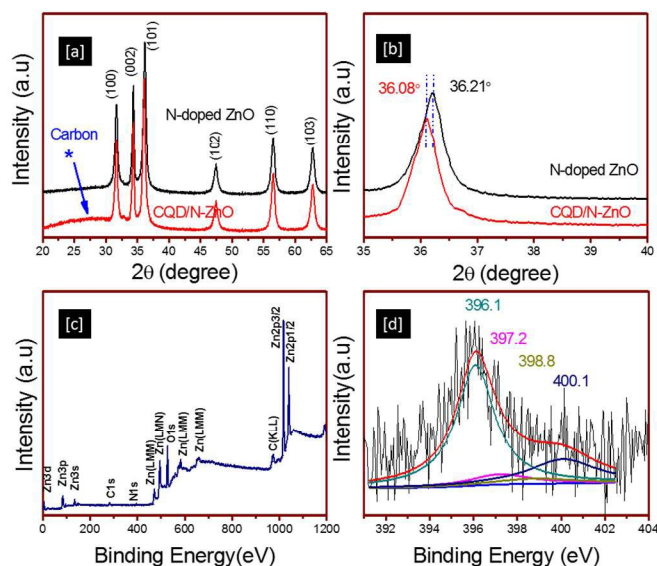

Figure 1. (a-b) XRD patterns of N-doped ZnO and CQD/N-ZnO composites. (c) XPS survey scan and (d) high resolution N 1s core spectrum of CQD/N-ZnO composite.

The nano-Raman spectroscope was performed to check the occurrence of Raman-active modes both phases of CQD and ZnO in CQD/N-ZnO composite, as shown in Fig 2a. The Raman-active modes of ZnO at 331 cm^{-1}, 434 cm^{-1}, and 580 cm^{-1} were related to the second-order scattering arising from zone-boundary phonons 2E2, E2 (high) and the polar symmetry modes A1 (LO) [15], respectively. Similarly, the occurrence of carbon related Raman-active modes of graphite (G) and defect (D) bands were observed at 1340 cm^{-1} and 1600 cm^{-1}, respectively, suggesting the presence of CQD and ZnO related Raman active modes in CQD/N-ZnO composite. Likewise, the existence of both phases in CQD/N-ZnO composite was confirmed by FT-IR spectroscopy, as shown in Fig. 2b. The broad absorption band of hydrogen bonded O–H stretching vibrations is appeared at ~3408 cm^{-1}; the other two peaks at ~2929 cm^{-1} and ~2862 cm^{-1} are assigned to the C–H stretching vibration. The asymmetric and symmetric vibrations of O–C–O peaks is seen at ~1619 cm^{-1} and ~1422 cm^{-1}; the occurrence of peaks at ~1129

cm^{-1} and ~902 cm^{-1} are related to the C–O bonds and epoxy groups; and the absorption bands at ~587 cm^{-1} is attributed to the stretching vibrations of Zn–O [4]. Furthermore, the UV–Vis absorption spectra of N-doped ZnO and CQD/N-ZnO composite were recorded, as shown in Fig. 2c-d. The representative absorption peak with a transition in the UV region was observed in both samples due to the bandgap transition of ZnO semiconductor. However, CQD/N-ZnO composite shows a continuous wide absorption from UV to visible region until 600 nm along with a slight shift in the bandgap energy to the lower region when compared with N-doped ZnO (Fig. 2d). Thus, the UV and FTIR results provide an additional support that CQDs have been successfully decorated on ZnO crystals, which is in agreement with the XRD and Raman results.
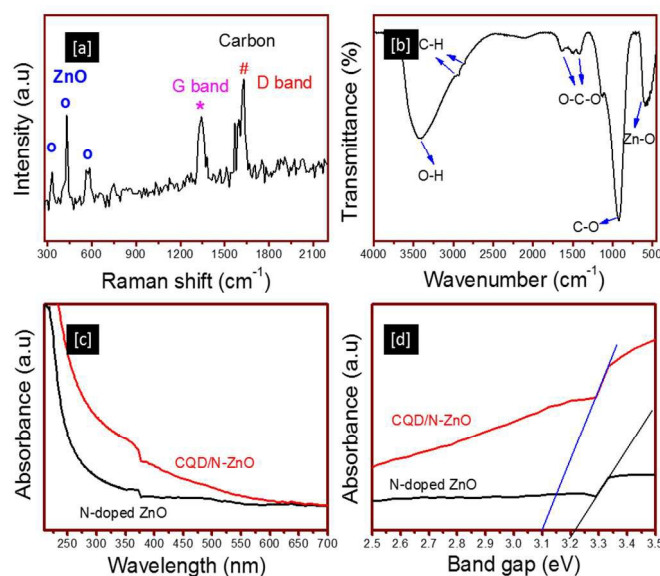

Figure 2. The Raman (a), FTIR spectrum (b) of CQD/N-ZnO composite and (c-d) UV-Vis absorption spectra of N-doped ZnO and CQD/N-ZnO composites.

Fig. 3(a-d) show the high magnified field emission scanning electron microscopy (FESEM) images and the respective EDS spectra of N-doped ZnO and CQD/N-ZnO composites. The size and shape of N-doped ZnO seems to be spherical shaped nanoparticles (~25 nm) dispersed throughout the sample, as shown in Fig. 3(a). Similarly, there is no considerable changes in the particle size, in case of CQD/N-ZnO photocatalyst in Fig. 3(c). However, the EDS spectra of CQD/N-ZnO shows the existence of zinc, oxygen, carbon and nitrogen that strongly confirms the presence of both phases of CQD and ZnO and it was further confirmed by TEM images. Fig. 3(e-f) shows the TEM and HRTEM image of CQD/N-ZnO composites. The particle sizes of N-doped ZnO crystal and pure CQD (Fig. S2) were found to be ~25 and 2.5 nm, respectively. Insets in Fig. 3(f) show the HRTEM image of CQD/N-ZnO composites and the lattice spacing were measured to be ~0.26 nm for ZnO and ~0.32 nm for carbon [4]. Based on the above results, it can be easily concluded that the CQD/N-ZnO composite is composed of CQDs and ZnO phases.

The photocatalytic activities of the N-doped ZnO and CQD/N-ZnO composites were evaluated for the photodegradation of malachite green (MG) dye under different light sources. In general, the absorption spectrum of MG dye consists of three peaks, a major peak was positioning at 612 nm and other two minor peaks were at 418

and 310 nm (Fig. S3). In order to monitor the degradation characteristic of MG dye, absorption peak appeared at 612 nm was considered rather than the other minor peaks, for accuracy. Fig. 4a shows the degradation efficiency graph of pure MG dye, N-doped ZnO and CQD/N-ZnO composites under the naturally available daylight irradiation. The degradation efficiency of 60% and 100% was measured after 30 min of daylight irradiation for N-doped ZnO and CQD/N-ZnO composites, respectively, while ~8% of MG dye degradation was noticed without catalyst (Fig. S3). This result demonstrated that CQD/N-ZnO composite shows a dramatic photocatalytic performance under daylight irradiation and it required just 30 min to degrade entire MG dye molecules.

photocatalytic performance: (1) both N-doping and CQD are being act as an electron reservoir, which will efficiently separate the photogenerated electron–hole pairs, and ultimately hinder the charge recombination to generate photo-reactive sites [14,19,21]; (2) a stronger electronic coupling of π electrons of carbon with the conduction band of ZnO is applicable, since the work-function of CQDs (−4.5 eV) is placed just below the conduction band energy of ZnO at −4.05 eV, leading to the up-conversion (Fig. S5) [5] and to extend the absorption capability into longer wavelength region [18]. Therefore, it is concluded that the enlarged visible-light absorption ability of ZnO crystal due to the N-doping [11,22] and CQD [5-7].
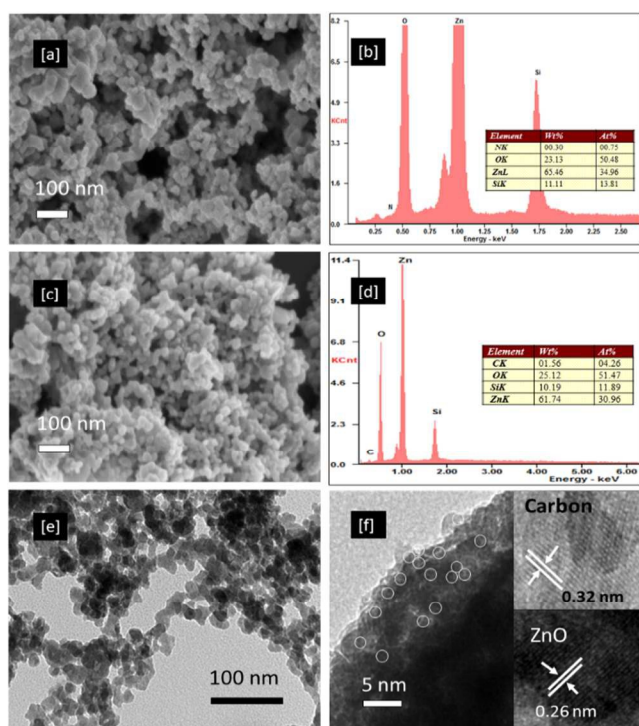

Figure 3. FESEM and SEM-EDS spectra of (a-b) N-doped ZnO and (c-d) CQD/N-ZnO composites [Inset: elemental composition data]. TEM image (e) and HRTEM image (f) of CQD/N-ZnO composites and the insets are the lattice space values of carbon and ZnO.

To validate the photocatalytic performance of CQD/N-ZnO composites, photodegradation percentage of CQD/N-ZnO composite was compared with other recent reports related to the CQD covered metal oxide photocatalysts. For instance, CQD/α-Fe$_2$O$_3$ photocatalyst destroys methylene blue [MB] dye in 90 min by adding H$_2$O$_2$ under visible light [16]. CQD/ZnO heterostructure disclosed ~80% degradation of RhB dye even after 2 h of UV light irradiation [17]. Similarly, C/TiO$_2$ photocatalyst needed at least 4 h of visible light irradiation to decompose ~80% of methyl orange dye [18]. Also, ZnO/graphene photocatalyst shows around 90% degradation of MB dye in 40 min under UV light [19]. TiO$_2$/C-dots photocatalyst needs at least 4h to degrade MB dye under visible light [13], and just 90% degradation of MB dye was resulted in 4h under near IR light with CQDs/Cu$_2$O [20]. Therefore, based on these information, we concluded that the superior photocatalytic performance of CQD/N-ZnO composite primarily from the combinational effect of both CQD and N-doping characteristics (Fig. S4). It holds the following possible reasons to enhance the
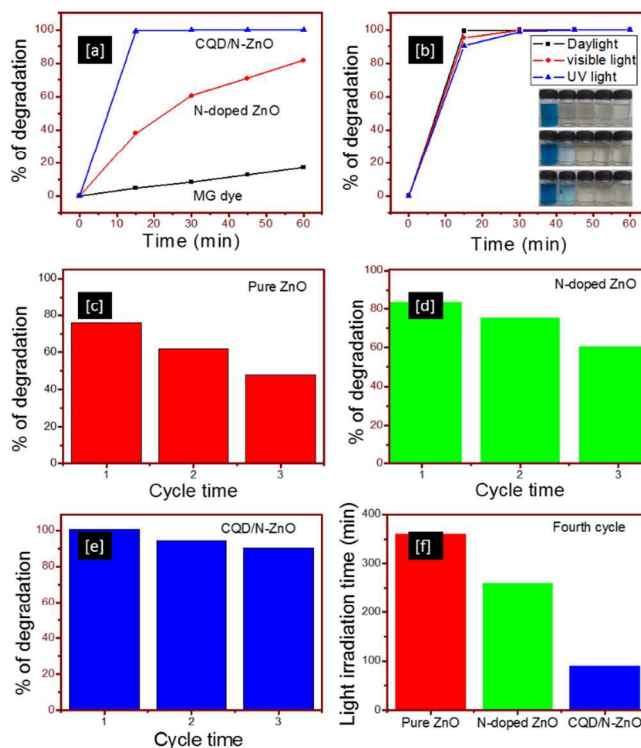

Figure 4. (a) Photocatalytic degradation on MG dye solution under daylight irradiation with respect to different photocatalysts and (b) photocatalytic degradation of MG dye under different light sources [Insets: the photographs of MG dye solution taken after regular interval of 0, 15, 30, 45 and 60 min under different light sources]. Photostability graphs of (c) pure ZnO, (d) N-doped ZnO and (e) CQD/N-ZnO composite under daylight irradiation in three cycle runs. (f) Fourth cycle performance of pure ZnO, N-doped ZnO and CQD/N-ZnO photocatalysts on MG dye degradation under daylight irradiation.

The photocatalytic performance of CQD/N-ZnO composites was further interrelated with other common light sources of UV and visible light, as shown in Fig. 4b. Irrespective of light sources, CQD/N-ZnO composites degrades an entire dye molecules within 30 min of light illumination. However, as seen in Fig 4(b) that a slight disparity in the percentage of degradation was noticed after 15 min of light exposure of UV (90%), visible (95%), and daylight sources (99%). These results were consistent with the photographs (insets in Fig. 4b) of the respective dye solution collected after the intervals of 15 min under different light irradiation. Here, a slight green shade is still appears in both UV and visible light irradiated samples (after 15 min), whereas, no such noticeable shade detected in daylight irradiated sample. At the same time, N-doped ZnO photocatalyst

required more than 60 min to degrade at least 80% of MG dyes upon daylight irradiation with a gradual decrease in colour shade, as seen in supporting information (Fig S6). Thus, we concluded that the CQD/N-ZnO photocatalyst exhibits a rapid degradation of MG dye solution, regardless to the light sources. In specific, a rapid photocatalytic performance of CQD/N-ZnO under daylight irradiation makes us to recommend to be a suitable candidate for the industrial wastewater treatment, since it is more effective towards the naturally available daylight rather than a specific light source to treat huge volume of wastewater in industry.

For industrial perspective, the anti-photocorrosion is an important characteristic for continuous usage of catalyst in dye degradation. Hence, the repeated experiments were conducted with pure ZnO, N-doped ZnO and CQD/N-ZnO composites and results indicated that CQD/N-ZnO composites was a relatively stable photocatalyst to be reused as an effective daylight photocatalyst. Fig. 4(c-e) show the successive experimental results of pure ZnO, N-doped ZnO and CQD/N-ZnO composites with three cycle under daylight irradiation for 60 min. The photocatalytic efficiency of pure ZnO decreased drastically from 75% (cycle 1) to 47% (cycle 3), while relatively lesser decreasing trend was observed in N-doped ZnO (83% to 60%) and CQD/N-ZnO composites (100% to 91%). The reduction in the degradation efficiency of CQD/N-ZnO composites probably due to the mass loss percent of photocatalyst during each cycle. It means that after each cycle, the photocatalyst was recovered by centrifuging, washing and reuse for a next cycle. However, the expected mass loss is lower than 2 to 3% by weight per cycle. In addition, 4th cycle experiment was carried out to investigate the total time requirement for degrading the MG dye molecules to the maximum, as shown in Fig. 4f. It was found that CQD/N-ZnO composite required just 90 min to degrade the MG dye completely in the fourth cycle beyond the weight loss, while N-doped ZnO proceeded with 4.2 h to degrade around 90% of MG dye under daylight irradiation. On the other hand, pure ZnO deteriorates to the extent of more than 6 h with 80% of dye degradation. This result strongly confirms the supressed photocorrosion offered by the CQDs, which could effectively inhibits the photocorrosion. It was verified with the TEM images and XRD spectra of photocatalysts after 4th successive experiments. Based on the TEM images, it can be clearly seen that the size and shapes were remain unchanged in case of CQD/N-ZnO photocatalyst, while wire-like morphologies were observed for N-doped ZnO (Fig S7). This observation was further confirmed by XRD measurements, the appearance of new XRD peaks at 27.6°, 32.7°, 59.3° and 60.3° representing the degradation of ZnO crystals leading to the formation of $Zn_5(OH)_6(CO_3)_2$ phase (Fig S7). Thus, these results indicate the coverage of CQDs could be act as a shield to preserve the ZnO crystals away from the photocorrosion.

In conclusion, naturally available daylight source was used to investigate photocatalytic response of CQDs decorated N-doped ZnO photocatalyst on the aqueous MG dye. It was recognized that a wider range of light excitation capability of CQD/N-ZnO can facilitate the higher separation efficiency, increase in the number of photo-reactive sites and with the suppressed photocorrosion, leading to suggest as a promising photocatalyst for wastewater treatment in industry.

Notes and references

1. S. Chakrabarti, and B. K. Dutta, *J. Hazard. Mater.,* 2004, **112**, 69-–78.
2. M. K. Lee, and H. F. Tu, *J. Electrochem. Soc.,* 2008, **155**, D758–62.
3. J. B. Mu, C. L. Shao, Z. C. Guo, Z. Y. Zhang, M. Y. Zhang, P. Zhang, B. Chen, and Y. C. Liu. *ACS Appl. Mater. Interfaces,* 2011, **3**, 590-96.
4. Y. Li, B. P. Zhang, J. X. Zhao, Z. H. Ge, X. K. Zhao, and L. Zou, *Appl. Surf. Sci.,* 2013, **279**, 367–73.
5. H. Yu, H. C. Zhang, H. Huang, Y. Liu, H. T. Li, H. Ming, and Z. H. Kang, *New J. Chem.,* 2012, **36**, 1031-35.
6. C. H. Kim, B. H. Kim, and K. S. Yang, *Carbon,* 2012, **50**, 2472-81.
7. X. Wang, L. Cao, F. S. Lu, M. J. Meziani, H. T. Li, G. Qi, B. Zhou, B. A. Harruff, F. Kermarrec, and Y. P. Sun, *Chem. Commun.,* 2009, **25**, 3774-76.
8. K. Dai, G. Dawson, S. Yang, Z. Chen, and L. Lu, *Chem. Eng. J.,* 2012, **191**, 571-78.
9. P. Muthirulan, M. Meenakshisundararam, and N. Kannan, *J. Adv. Res.,* 2013, **4**, 479-84.
10. S. S. Shinde, C. H. Bhosale, and K. Y. Rajpure, *J. Photochem. Photobiol. B*, 2012, **113**, 70–77.
11. H. T. Li, Z. H. Kang, Y. Liu, S. T. Lee, *Mater. Chem.,* 2012, **22**, 24230–53.
12. P. Uthirakumar, S. Muthulingam, B. D. Ryu, J. H. Kang, A. Periyasamy, M. Prabakaran, and C. H. Hong, *Curr. Nanosci.,* 2013, **9**, 335-40.
13. P.B. Ashwini, D.S. Shivaram, P.W. Rupali, K.N. Latesh, and B.K. Bharat, *Green Chem.,* 2012, **14**, 2790–98.
14. X. Zong, C. Sun, H. Yu, Z.G. Chen, Z. Xing, and D. Ye, *J. Phys. Chem. C,* 2013, **117**, 4937–4942.
15. H. M. Cheng, K. F. Lin, H. C. Hsu, C. J Lin, L. J. Lin and W. F. Hsieh, *J. Phys. Chem. B,* 2005, **109**, 18385-90.
16. B. Y. Yu, and S. Y. Kwak. *J. Mater. Chem.,* 2012, **22**, 8345-53.
17. Y. Li, B. P. Zhang, J. X. Zhao, Z. H. Ge, X. K. Zhao, and L. Zou, *Appl. Surf. Sci.,* 2013, **279**, 367– 73.
18. L. Zhao, X. Chen, X. Wang, Y. Zhang, W, Wei, Y. Sun, M. Antonietti, and M. M. Titirici, *Adv. Mater.,* 2010, **22**, 3317–21.
19. T. Xu, L. Zhang, H. Cheng, and Y. Zhu, *Appl. Cat. B: Environ.,* 2011, **101**, 382–87.
20. H. T. Li, R.H. Liu, Y. Liu, H. Huang, H. Yu, H. Ming, S. Y. Lian, S. T. Lee, and Z. H. Kang, *J. Mater. Chem.,* 2012, **22**, 17470-5.
21. Y. Qiu, K. Yan, H. Deng, and S. Yang, *Nano Lett.,* 2012, **12**, 407–13.

a Nanoscience Center for Optoelectronic and Energy Devices [Nano-COED], Department of Chemistry, Sona College of Technology, Salem, Tamilnadu 636 005, India

b School of Advanced Materials Engineering and Research Center of Advanced Materials Development, Chonbuk National University, Jeonju 561-756, South Korea

*Corresponding author: Tel: +82-63-270-2292;

E-mail: uthirakumar@gmail.com (P. Uthirakumar); ihlee@gmail.com (In Hwan Lee)